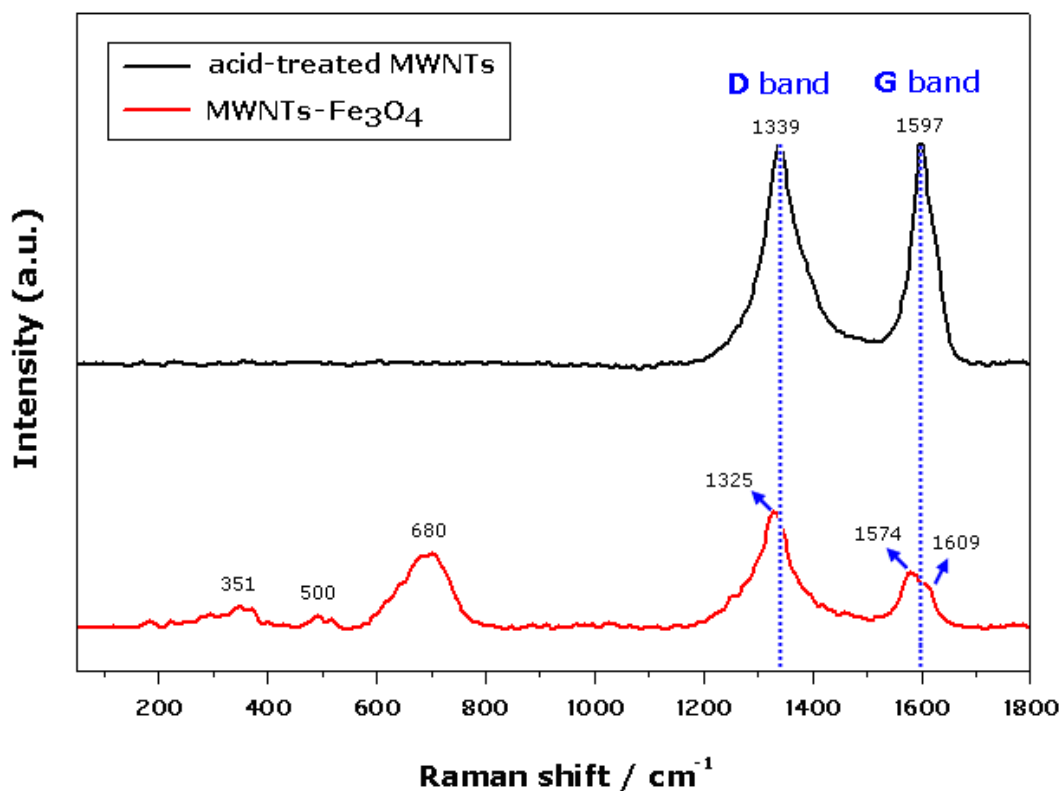
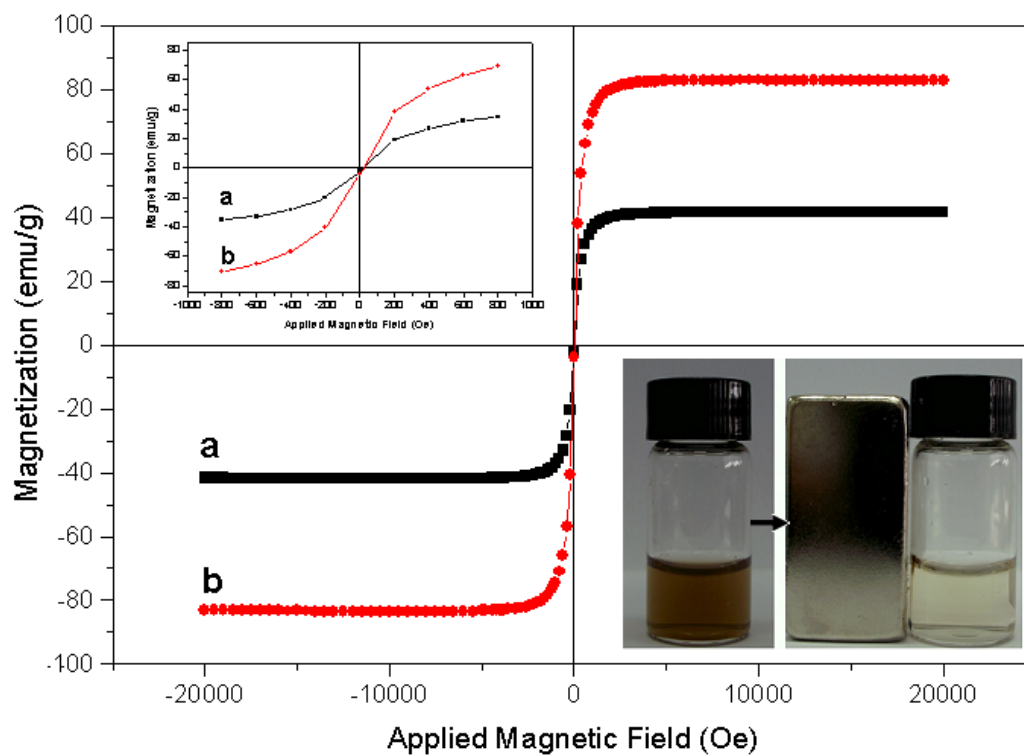


**Fig. S1** The XRD pattern of magnetic MWNTs-Fe<sub>3</sub>O<sub>4</sub> nanomaterials.



**Fig. S2** The Raman spectra of acid-treated MWNTs and magnetic MWNTs-Fe<sub>3</sub>O<sub>4</sub> nanomaterials. The Raman spectrum of acid-treated MWNTs showed the similar intensity of D bands (1339 cm<sup>-1</sup>) in comparison to G bands (1597 cm<sup>-1</sup>), which was due to the presence of more defects at the surface of MWNTs. A small shift in G band and D band peaks was observed in the case of magnetic MWNTs-Fe<sub>3</sub>O<sub>4</sub> nanocomposites. Along with a shift in G and D bands, the characteristic band centered at 680 cm<sup>-1</sup> was observed at lower Raman shift values in the magnetic MWNTs-Fe<sub>3</sub>O<sub>4</sub>. This band indicated that the magnetite nanoparticles were successfully immobilized on the surface of MWNTs.



**Fig. S3** The hysteresis loops of a) MWNTs-Fe<sub>3</sub>O<sub>4</sub> and b) Fe<sub>3</sub>O<sub>4</sub> nanoparticles. The two nanoparticles exhibited a superparamagnetic behavior, that is, no remanence was detected at room temperature (above inset). Meanwhile, the PL-MWNTs-Fe<sub>3</sub>O<sub>4</sub> nanomaterials in their homogeneous dispersion showed fast moment to the applied magnetic field (2000 Oe) (below inset).

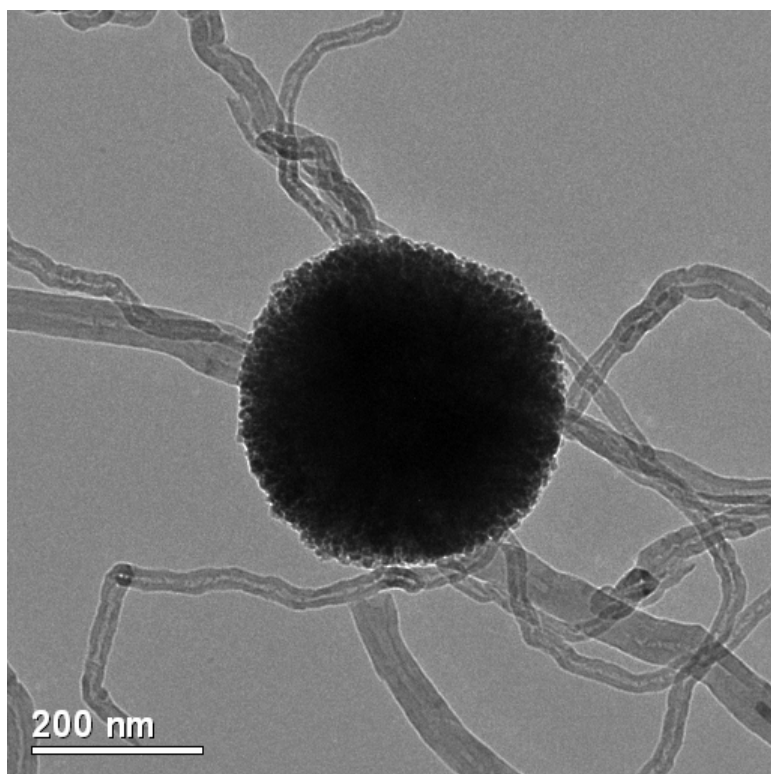


**Fig. S4** Representative TEM image of the synthesized magnetic MWNTs-Fe<sub>3</sub>O<sub>4</sub> nanomaterials with octopus claw-like nanostructures using NaAc.

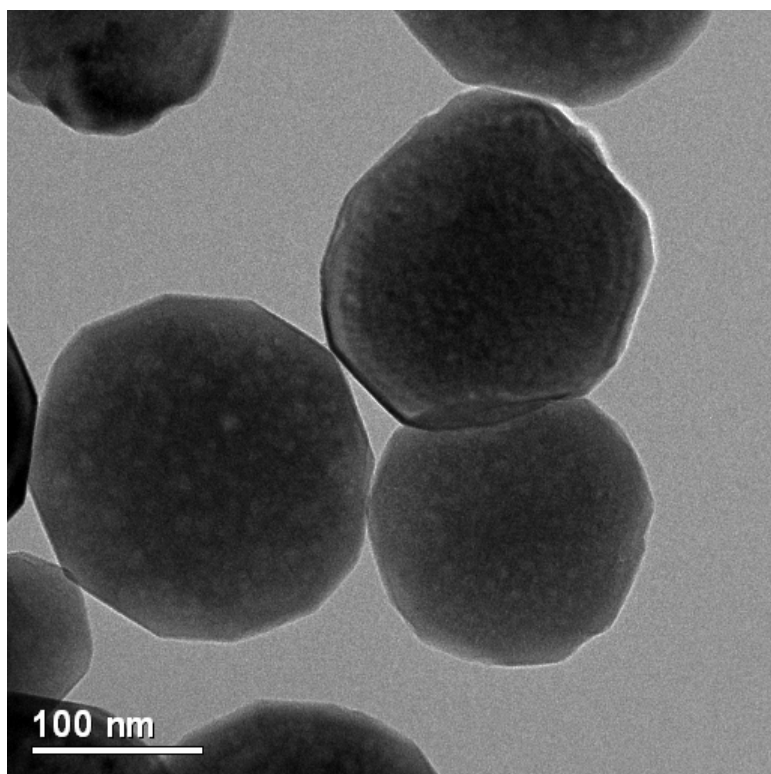


**Fig. S5** Representative TEM image of the synthesized magnetite nanoparticles.

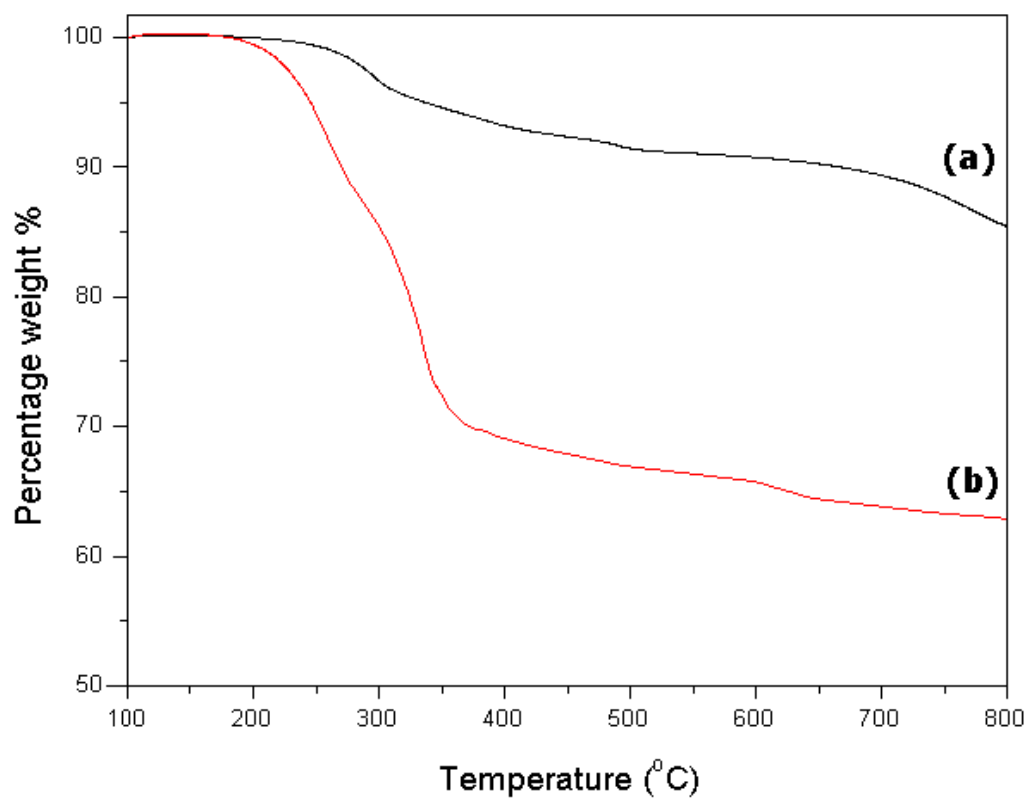


**Fig. S6** TGA of (a) MWNTs-Fe<sub>3</sub>O<sub>4</sub> and (b) PL-MWNTs-Fe<sub>3</sub>O<sub>4</sub>. The result indicated that about 22 wt% polyethylene glycol based on the total weight of the MWNTs-Fe<sub>3</sub>O<sub>4</sub> could be covalent.

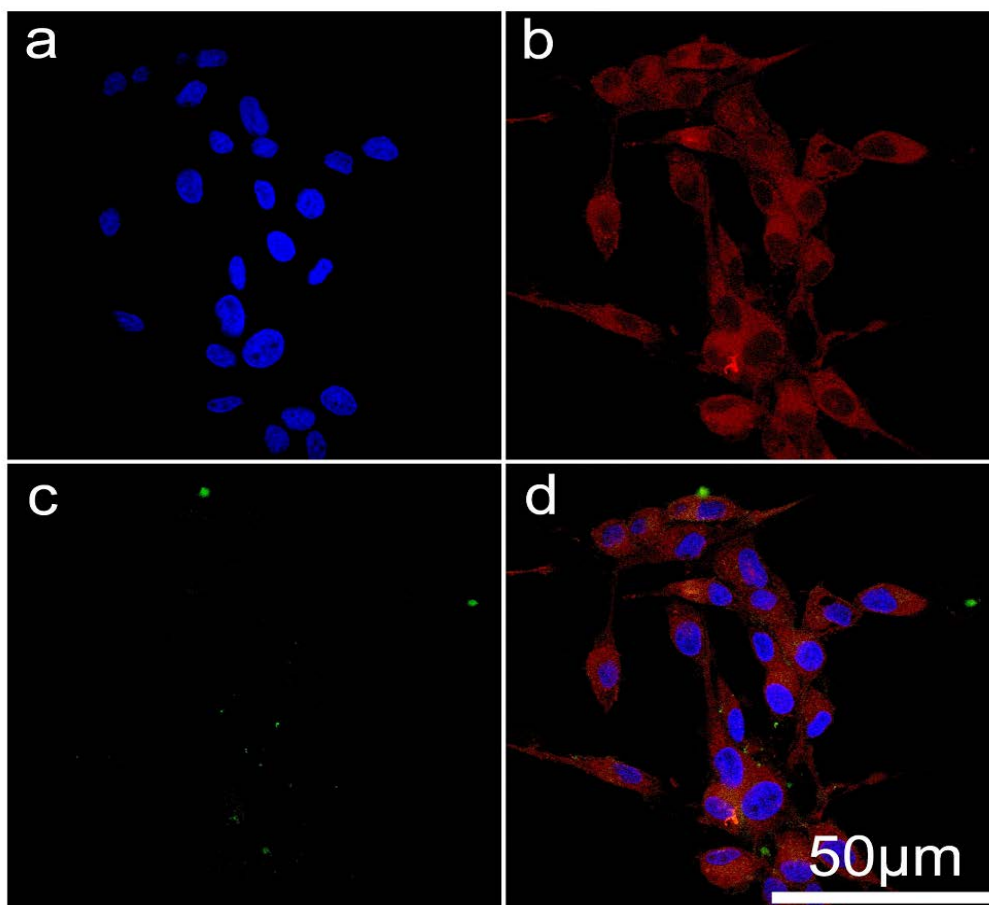


**Fig. S7** Confocal fluorescence microscopy images of FITC uptake by U87 cancer cells. The control experiment was investigated by using FITC instead of FITC-labeled nanomaterials in our study, hardly any green fluorescence of FITC was observed, which showed that FITC-labeled MWNTs-Fe<sub>3</sub>O<sub>4</sub> nanomaterials could be used as fluorescent probes for cell imaging.

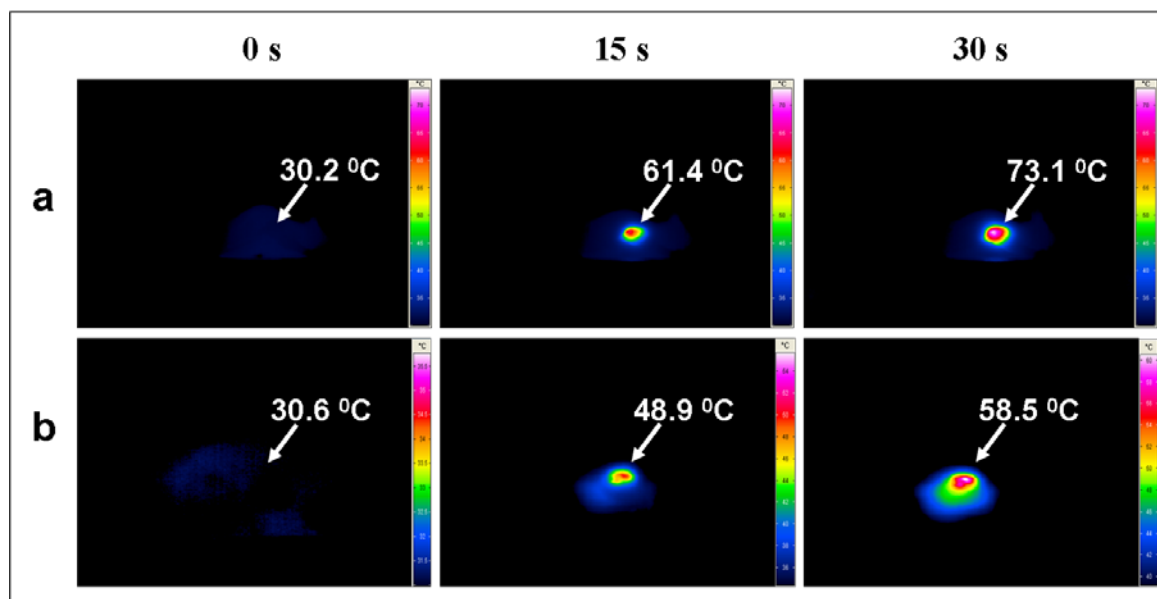


**Fig. S8** Infrared thermal images of (a) PL-MWNTs-Fe<sub>3</sub>O<sub>4</sub>-injected and (b) PL-MWNTs-injected U87 tumor sample at different time points (0, 15, 30 sec) under NIR laser irradiation.



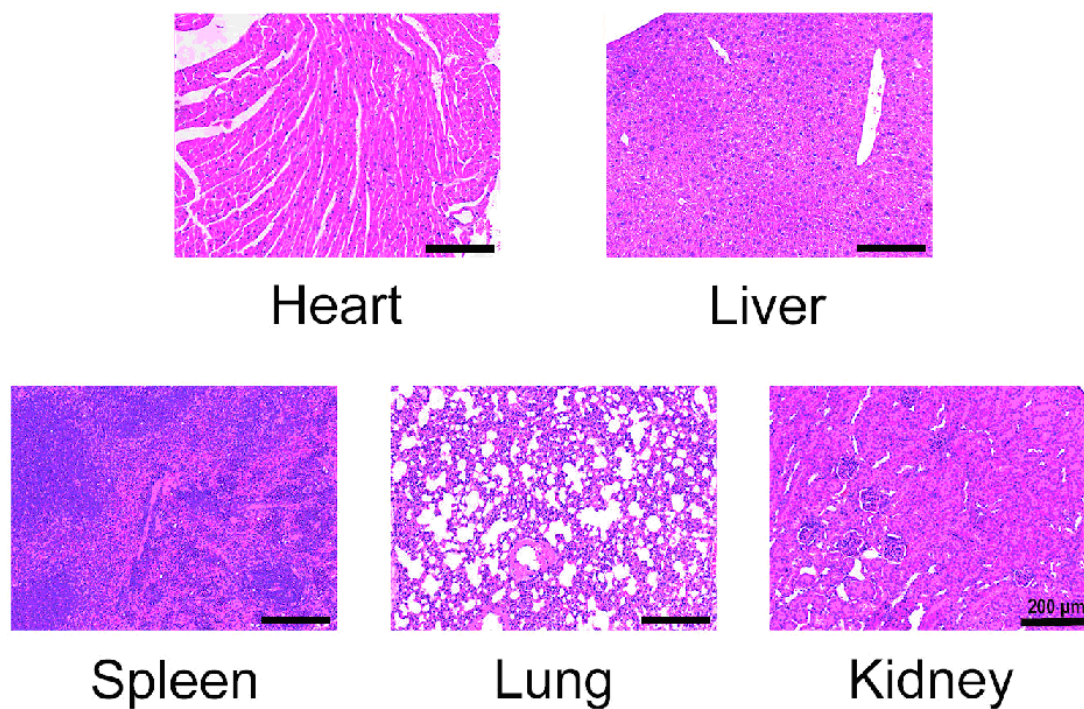


**Fig. S9** Histological analysis of surviving mice following PL-MWNTs-Fe<sub>3</sub>O<sub>4</sub> nanomaterials-based photothermal therapy reveals no overt pathological changes. No significant lesions were detected.